Computational Performance of GTD-RT Applied for Evaluation of Electromagnetic Scattering on Rough Surfaces

Asmaa E. Farahat and Khalid F. A. Hussein

Microwave Engineering Department
Electronics Research Institute, Cairo, 11843, Egypt
asmaa@eri.sci.eg, khalid_elgabaly@yahoo.com

Abstract ─ In this paper, a new robust computational method that applies the geometrical theory of diffraction (GTD) in conjunction with the ray tracing (RT) technique is developed to evaluate the electromagnetic scattering pattern due to a plane wave represented as beam of parallel rays incident on a rough surface of quite arbitrary statistical parameters. The development of the proposed technique is explained in detail taking into consideration the generation of the geometrical model of the rough surface. The Fresnel reflection model is applied under the assumption of arbitrary electrical and optical properties of the rough surface material. Also the polarization of the plane wave primarily incident on the rough surface is taken into consideration. The algorithm developed in the present work accounts for multiple bounces of an incident ray and, hence, it can be considered arbitrary higher-order GTD-RT technique. The accuracy of the obtained results is verified through the comparison with the experimental measurements of the scattering pattern of a light beam incident on rough sheets with specific statistical properties. The numerical results of the present work are concerned with investigating the dependence of the scattering pattern on the surface roughness, refractive index, angle of incidence, and the resolution of the geometric model of the rough surface. Also, it is shown that, for limited resolution of the rough surface model, the accuracy of the calculated scattered field depends on the angle of incidence of the primary beam and the surface roughness.

Index Terms ─ GTD-RT technique, polarization, random rough surfaces, scattering measurement.

I. INTRODUCTION

Studying electromagnetic (EM) scattering from random rough surfaces, especially in the visible and infrared spectral range, is of great importance for many applications and scientific research purposes. The characterization of rough surfaces through the investigation of the EM and light scattering finds wide fields of scientific research [1-8]. One of the most important applications is the optical tomography, in which the scattering patterns for a beam incident on an objective material provide extensive information such as the surface roughness and optical properties. The characterization of the materials and devices used in VLSI manufacturing is usually accomplished by studying the light scattered from the surfaces of such constituents. Both theoretical and experimental investigation of EM scattering from rough surfaces has great importance in many scientific, commercial, and military applications such as the earth remote sensing for studying the ocean surface and the terrain at long length scales [9-11].

Some analytic and semi-analytic techniques have been proposed for evaluating the EM scattering from rough surfaces [12-26]. These include (i) the small-amplitude perturbation theory, in which the scattered field is expanded in powers of the surface profile function through linear terms, (ii) the Kirchhoff approximation, in which the scattering is treated as reflection from the plane tangent to the surface at each point, (iii) the extinction theorem in which the scattering equations, based on this theorem are solved numerically and, finally, (iv) the techniques based on the Rayleigh scattering equation. In [21], the relationship between the pattern of the scattered light and the statistical properties of the scattering surface given by Beckmann–Kirchhoff theory is utilized to measure the surface roughness through an iterative procedure proposed by inverting this relationship, to retrieve the height autocorrelation function. In [22], different ways in which light scatter can be used to measure surface roughness are described. It provides reviews of the most common types of light scattering used for this purpose. These are the angle resolved scatter and the total integrated scatter. In the first type, the light scattered in the different directions is measured and studied, but in the second type, the light scattered in all the directions except for the specular direction is measured and analyzed. In [23], the scattering of electromagnetic waves from a rough surface interface between the free space and a dielectric medium is evaluated using mathematical and numerical treatment. The boundary values of the field and its

Submitted On: July 23, 2019
Accepted On: July 6, 2021

https://doi.org/10.47037/2020.ACES.J.360601

normal derivative on the interface are obtained using the extinction theorem. Then, the angular distribution of the ensemble average of reflected and transmitted field intensities are calculated. In this method, one-dimensional profiles for the rough surface are generated through a Monte Carlo method to solve the scattering equations numerically. In [24], a numerical solution of the reduced Rayleigh equation for the scattering of light from two-dimensional penetrable rough surfaces is achieved. The pattern of the light scattered from the surface is calculated by considering a horizontally or vertically polarized light wave incident on two-dimensional Gaussian or cylindrical rough surfaces of either isotropic or anisotropic statistical properties. The work of [15] provides physical optics solution for the scattering of a partially-coherent wave from a rough surface of dielectric material. A summary of other techniques used for the assessment of electromagnetic scattering from rough surfaces is provided in [16]. The methods reviewed in [16] include the Meecham–Lysanov method, phase-perturbation method, small-slope approximation, operator expansion method, tilt-invariant approximation, local weight approximation, weighted curvature approximation, Wiener–Hermite approach, unified perturbation expansion, full-wave approach, improved Green's function methods, volumetric method and integral equation method.

The present paper applies the Geometrical Theory of Diffraction (GTD) in conjunction with the Ray Tracing (RT) to account for scattering of optical waves and other electromagnetic waves from rough surfaces. Such GTD-RT technique accounts for higher order scattering by considering multiple bounces of the ray incident on a rough surface. Moreover, the Fresnel reflection and transmission coefficients are calculated to take into consideration the effect of the material of the rough surface. This method is applicable for random rough surfaces of both metallic and dielectric materials with quite arbitrary statistical parameters. The proposed GTD-RT technique is fully numerical and avoids the approximations encountered in the analytical or semi-analytical techniques that result in significant inaccuracies (except for the high frequency formulation which is the spirit of the ray theory).

The numerical results for the scattering pattern evaluated using the GTD-RT method is investigated through experimental verification. The polarization of the plane wave incident on the rough surface is taken into consideration. The present work investigates the dependence of the accuracy of the resulting scattering pattern on the resolution of the geometric model of the rough surface. Also, it studies the dependence of the accuracy of the calculated scattered field on the angle of incidence of the primary beam and the surface roughness.

II. GENERATION OF RANDOM ROUGH SURFACE MODEL

In this section we describe a simple spatial-domain method to generate a random rough surface with predetermined statistical properties. The most important statistical properties of such a random surface are the mean value of the surface height, h_{mean}, the root-mean-squared-height h_{rms}, and the correlation length between the heights of the neighboring points on the surface, L_c.

Let the dimensions of the surface be $L_x \times L_y$ which is discretized to $Q_x \times Q_y$ points (vertices) along x and y directions, respectively. The correlation lengths are L_{cx} and L_{cy} along x and y directions, respectively. The coordinates of each point in surface are (x, y, z), where z is the random height whereas x and y represent a uniform horizontal grid. The horizontal distances between two adjacent points are Δx and Δy along x and y directions, respectively. The roughness degree of such a surface depends on the ratio between h_{rms} and the correlation length. For a square isotropic surface, $L_{cx} = L_{cy} = L_c$, $L_x = L_y = L$, $Q_x = Q_y = Q$, and $\Delta x = \Delta y = \Delta$. For such a surface let N_{Lc} be the number of the surface points taken along the correlation length and, hence, L_c can be calculated as follows:

$$L_c = (N_{Lc} - 1)\,\Delta. \tag{1}$$

In this case the degree of roughness R_D or, simply, the roughness can be defined as:

$$R_D = \frac{2h_{rms}}{L_c}. \tag{2}$$

To generate a rough surface numerically, a two-dimensional array of discrete Gaussian random numbers with zero-mean, $\mu = 0$, and a standard deviation $\sigma = h_{rms}$ are generated. These random numbers represent the heights of the discrete points on the random surface. In this manner the heights are uncorrelated. To get a rough surface model with a specific correlation length, a Savitzky-Golay filter with a correlation window size of N_{Lc} is applied to smooth the rows and then the columns of the generated array of random numbers [27]. The mean value of the resulting (smoothed) array is subtracted from the values of the array elements which are then scaled to get their standard deviation equal to the required root-mean-squared height of the surface.

III. EVALUATION OF OPTICAL WAVE SCATTERING ON RANDOM ROUGH SURFACES

This section is concerned with the evaluation of the optical scattering from random rough surfaces with arbitrary statistical parameters using the GTD in conjunction with the RT technique. The geometrical model of the rough surface is created as described in Section 2 such that the plane of incidence is parallel to

x-z plane. The plane wave polarization is considered vertically polarized (V-polarized) if the electric field lies completely in the plane of incidence and is considered horizontally polarized (H-polarized) if the electric field lies completely in the plane parallel to the x-y plane.

A. Applicability of the GTD-RT technique for optical scattering on rough surfaces

For an optically rough surface model, the following conditions are practically satisfied. To get accurate numerical assessment of the optical wave scattering on such a surface using the GTD-RT technique, the following condition should be satisfied [25]:

$$\lambda \ll L_c\sqrt{1+R_D^2}, \qquad \lambda \gg \Delta. \tag{3}$$

If the conditions given by (3) are satisfied, the GTD-RT technique can be applied to evaluate the scattering of an optical ray (or beam of rays) incident on such rough surface model.

B. Application of GTD-RT for assessment of scattering of parallel rays on rough surfaces

This section provide a detailed description of the proposed GTD-RT technique when applied to evaluate the optical and EM scattering due to a plane wave illuminating a rough surface as shown in Fig. 1. The incident plane wave is represented by a number of rays; each ray is associated with an amount of power that is to be calculated so as to satisfy uniform power distribution over the transverse plane of the incident wave. The phase associated with each of the scattered rays is obtained by calculating the total distance travelled during ray tracing. The rough surface absorption or reflectance is evaluated by calculating the Fresnel coefficients at the point of incidence. Finally, a method is proposed to calculate the scattering pattern over the upper half space. Both first order and higher order ray tracing are described through systematic algorithm facilitated to be applied as a simulation tool for optical and EM scattering on rough surface.

The random rough surface is discretized to a grid of vertices arranged uniformly in the x and y directions and separated by steps Δx and Δy, respectively. The number of vertices along x and y directions are P and Q, respectively. Each vertex of this uniform grid has a random height $z_{p,q}$, where the indices p and q refer to the vertex row and column of the grid in the x and y directions, respectively. Thus, the position vector of a vertex on the rough surface can be expressed as:

$$V_{p,q} = x_{p,q}\,\hat{a}_x + y_{p,q}\,\hat{a}_y + z_{p,q}\,\hat{a}_z, \tag{4}$$

where,

$$x_{p,q} = p\Delta x\,, \qquad y_{p,q} = q\Delta y. \tag{5}$$

Each vertex of the gird representing the rough surface is connected with the adjacent vertices using triangular meshing. The normal vector at each vertex of the surface is the average of the normal vectors of the adjacent triangular patches sharing this vertex. The procedure to apply the proposed GTD-RT method is detailed in the following subsections.

B.1 Ray representation of the incident plane wave

The vector propagation constant of the incident plane wave can be expressed as:

$$k_i = k_o\hat{a}_{k_i} = k_o\left(\hat{a}_x k_{i_x} + \hat{a}_z k_{i_z}\right), \tag{6}$$

where, k_o is the free space wavenumber, $\hat{a}_{k_i}$ is the unit vector in the direction of propagation, and,

$$k_{i_x} = \sin\theta_i\,, \qquad k_{i_z} = \cos\theta_i. \tag{7}$$

The incident plane wave is represented by a number of parallel rays by setting a ray incident on each vertex $V_{p,q}$ of the rough surface. Each ray is associated with an amount of power $\mathcal{P}_{i_{p,q}}$ which is determined so as to satisfy uniform power density distribution over the transverse plane. Without any loss in generality, it is assumed that the propagation unit vector of the plane wave $\hat{a}_{k_i}$, is always in the x-z plane (the squint angle is zero). Consider the transverse plane (normal to $\hat{a}_{k_i}$) that passes through the point $O_q = (0, y_{p,q}, 0)$. The transverse plane intercepts the plane $y = y_{p,q}$ in the line $\mathcal{L}_{i_q}$ that passes through the point O_q.

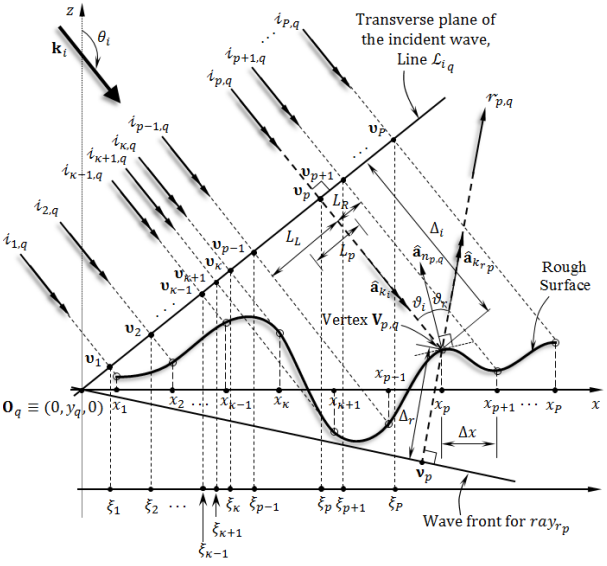

Fig. 1. The plane of incidence $y = (q-1)\,\Delta y$. Application of the ray tracing technique to calculate the scattering of plane waves on rough surfaces.

B.2 Calculating the power associating each of the incident rays

Starting from the 1st row of vertices of the mesh representing the rough surface and moving sequentially

to the Q^{th} row, the following procedure is applied to scan the vertices on the q^{th} row, $V_{p,q}$, sequentially from $p = 1$ to $p = P$:

1- From each vertex, $V_{p,q}$, draw a line perpendicular to the transverse plane of the incident wave, as shown in Fig. 1, and find the intersection point υ_p whose position vector relative to the point O_q is $\upsilon_p = (\xi_{p,q}, 0, \zeta_{p,q})$. This can be achieved as follows:

$$\upsilon_p \cdot \hat{a}_{k_i} = 0 = \xi_{p,q}\, k_{i_x} + \zeta_{p,q}\, k_{i_z}. \tag{8}$$

Let Δ_i be the distance from the intersection point υ_p to the vertex $V_{p,q}$; consequently, one has:

$$V_{p,q} = \upsilon_p + \Delta_{i_{p,q}}\, \hat{a}_{k_i}. \tag{9}$$

This relation can be split into the following scalar equations:

$$\xi_{p,q} = x_{p,q} - k_{i_x}\, \Delta_{i_{p,q}}, \tag{10a}$$

$$\zeta_{p,q} = z_{p,q} - k_{i_z}\, \Delta_{i_{p,q}}. \tag{10b}$$

Equations (8), (10a) and (10b) can be solved together to get $\Delta_{i_{p,q}}$, $\xi_{p,q}$ and $\zeta_{p,q}$ as follows. Substitute from (10a,b) into (8), one gets:

$$\Delta_i = x_{p,q} \sin\theta_i + z_{p,q} \cos\theta_i. \tag{11}$$

2- Define ξ_{max} as the maximum value of x-component of υ_p evaluated during the progress of scanning the vertices on the q^{th} row sequentially from $p = 1$ to $p = P$. Initially set $\xi_{max} = 0$, and define a flag variable $\Upsilon_{p,q}$ for the incident ray at this vertex.

3- With scanning the vertices on the q^{th} row moving from left to right, the index p increases by one for each vertex where the intersection point υ_p is calculated as described above and the value of ξ_{max} is updated; that is, if $\xi_{p,q} > \xi_{max}$, then this ray is considered active ($\Upsilon_{p,q} = 1$) and the ξ_{max} is updated as $\xi_{max} = \xi_{p,q}$. If $\xi_{p,q} \le \xi_{max}$, then the ray incident on this vertex is considered inactive ($\Upsilon_{p,q} = 0$), which means that the vertex (p, q) is shadowed from the incident wave by some part of the surface. Consequently, the ray $i_{p,q}$ does not contribute to the scattered field, which implies that the power associating this ray should be set to zero. Thus, as shown in Fig. 1, the area illuminated by each incident ray on the transverse plane are not equal and can be expressed as,

$$\Lambda_{p,q} = \tfrac{1}{2}(L_R + L_L)\, \Delta y, \tag{12}$$

where L_R is the distance between the point υ_p and the nearest right-hand point, υ_{p_R}, on the line $\mathcal{L}_{i_q}$ corresponding to an active ray, and L_L is the distance between the point υ_p and the nearest left-hand point, υ_{p_L}, corresponding to an active ray. Thus, one has:

$$L_R = \left|\upsilon_{p_R} - \upsilon_p\right|, \tag{13}$$

$$L_L = \left|\upsilon_{p_L} - \upsilon_p\right|. \tag{14}$$

Consequently, to get uniform power density on the transverse plane, the power associating each ray $\mathscr{P}_{i_{p,q}}$, should be proportional to $\Lambda_{p,q}$ and, hence, can be expressed as,

$$\mathscr{P}_{i_{p,q}} = \Lambda_{p,q}\, P_d\,, \tag{15}$$

where, P_d is the power density of the incident plane wave.

B.3 Calculating the directions of the reflected rays

The ray $i_{p,q}$ incident on the rough surface at the vertex $V_{p,q}$, makes an angle ϑ_i with $\hat{a}_{n_{p,q}}$, which is the unit vector normal to surface at this vertex. The reflected ray at the same vertex is $r_{p,q}$; it lies in the same plane of $\hat{a}_{k_i}$ and $\hat{a}_{n_{p,q}}$ and makes an angle $\vartheta_r = \vartheta_i$ with $\hat{a}_{n_{p,q}}$. Hence, the unit vector of the propagation constant $\hat{a}_{k_{r_p}}$ of the reflected ray ray_{r_p} can be determined as follows:

$$\hat{a}_{k_{r_p}} = \frac{1}{\left|\hat{a}_{k_i} - 2\left(\hat{a}_{k_i}\cdot\hat{a}_{n_{p,q}}\right)\hat{a}_{n_{p,q}}\right|}\Big[\hat{a}_{k_i} - 2\left(\hat{a}_{k_i}\cdot\hat{a}_{n_{p,q}}\right)\hat{a}_{n_{p,q}}\Big]. \tag{16}$$

The unit vector $\hat{a}_{k_{r_p}}$ can be written in terms of its components as follows:

$$\hat{a}_{k_{r_p}} = k_{rx_p}\hat{a}_x + k_{ry_p}\,\hat{a}_y + k_{rz_p}\,\hat{a}_z. \tag{17}$$

B.4 Calculating the phases of the reflected rays in the far zone

To calculate the phase associated with each scattered ray, the distance travelled by the ray should be evaluated. $\Delta_{r_{p,q}}$From each vertex, $V_{p,q}$, draw the normal to the wave front of the reflected ray as shown in Fig. 1. Find the intersection point ν_p whose position vector relative to the point O_q is $\nu_p = (\alpha_p, \beta_p, \gamma_p)$. This can be achieved as follows:

$$\nu_p \cdot \hat{a}_{k_{r_p}} = 0 = \alpha_p\, k_{rx_p} + \beta_p\, k_{ry_p} + \gamma_p\, k_{rz_p}. \tag{18}$$

Let $\Delta_{r_{p,q}}$ be the distance from the vertex $V_{p,q}$ to the intersection point ν_p. Thus,

$$\nu_p = V_{p,q} - \Delta_{r_{p,q}}\, \hat{a}_{k_{r_p}}. \tag{19}$$

This can be written in scalar equations as follows,

$$\alpha_p = x_{p,q} - k_{r_x}\, \Delta_{r_{p,q}}, \tag{20a}$$

$$\beta_p = y_{p,q} - k_{r_y}\, \Delta_{r_{p,q}}, \tag{20b}$$

$$\gamma_p = z_{p,q} - k_{r_z}\, \Delta_{r_{p,q}}. \tag{20c}$$

Solve equations (18), (20a), (20b) and (20c) together to get Δ_r, as follows:

$$\Delta_{r_{p,q}} = x_{p,q}\, k_{r_x} + x_{p,q}\, k_{r_y} + z_{p,q}\, k_{r_z}. \quad (21)$$

Thus, the phase associated with the $r_{p,q}$ can be expressed as,

$$\Delta\Phi_{p,q} = \frac{2\pi}{\lambda}\left(\Delta_{i_{p,q}} - \Delta_{r_{p,q}}\right). \quad (22)$$

B.5 Higher order scattering

An incident ray having its first collision with a vertex of the rough surface model may suffer higher order collisions at other vertices. A ray incident on a vertex $V_{p,q}$ may be subjected to higher order reflection if the reflected ray collides with the rough surface at another vertex. Figure 2 shows the geometry required to discuss the condition that such a reflected ray should satisfy to collide with the rough surface. The angle between the ray reflected at the vertex $V_{p,q}$ and the horizontal line, τ_r, can be expressed as:

$$\tau_r = \frac{\pi}{2} - \cos^{-1} k_{r_z}. \quad (23)$$

According to the geometry presented in Fig. 2, this ray will escape from other possible collisions with the rough surface if $\tau_r > \tau_D$, where τ_D is defined as,

$$\tau_D = \tan^{-1}\left(R_D - \frac{2z_{p,q}}{L_C}\right). \quad (24)$$

Thus, only the reflected ray that satisfies the following condition can probably collide with another point on the rough surface before going to the far zone causing second-order scattering:

$$\tau_r < \tau_D. \quad (25)$$

For optimization of the computational complexity the reflected rays not satisfying the condition (25) will not be checked for higher order reflections on the rough surface.

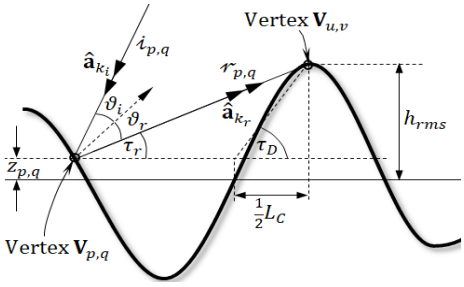

Fig. 2. Condition required to consider higher order reflection of an incident ray.

It is clear form (25) that a higher surface roughness causes larger number of rays to be subjected to higher order reflections. Only for those reflected rays that satisfy (25) the following procedure is applied.

The ray that has the t^{th} bounce at the vertex $V_{p,q}$ collides with the rough surface at the vertex $V_{u,v}$ if the following condition is satisfied:

$$\hat{a}_{k_r}^{(t)} \cdot \hat{a}_{p,q}^{u,v} = 1\,, \quad (26)$$

where $\hat{a}_{k_r}^{(t)}$ is the unit vector in the direction of the reflected ray due to the t^{th} bounce, and $\hat{a}_{p,q}^{u,v}$ is the unit vector in the direction from $V_{p,q}$ to $V_{u,v}$:

$$\hat{a}_{p,q}^{u,v} = \frac{V_{u,v} - V_{p,q}}{\left|V_{u,v} - V_{p,q}\right|}. \quad (27)$$

If the condition (25) is satisfied then this ray will have its $(t+1)^{th}$ bounce at the vertex $V_{u,v}$ as shown in Fig. 2. It should be noted that for each bounce of a ray, the direction of the reflected ray is calculated as described in Section III.B.3. The phase associating a ray arriving at the far zone can be calculated as follows:

$$\Delta\Phi_{p,q} = \frac{2\pi}{\lambda}\left(\Delta_{i_{p,q}} - \Delta_{r_{u,v}}\right) + \sum_{\nu=2}^{N_{O_{p,q}}} \frac{2\pi}{\lambda} D^{(\nu-1)}, \quad (28)$$

where $D^{(\nu-1)}$ is the distance travelled by the reflected ray between the $(\nu-1)^{th}$ and the ν^{th} bounce points on the rough surface at the $(\nu-1)^{th}$ bounce point, where $\nu \geq 2$, $N_{O_{p,q}}$ is the maximum number of considered bounces, which is equal to the order of GTD-RT technique.

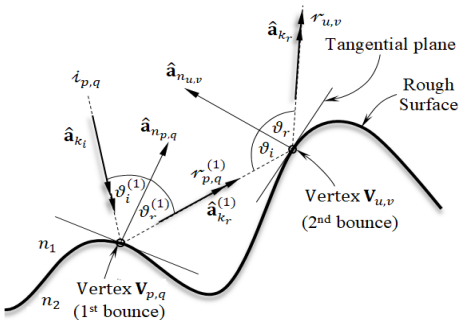

Fig. 3. Double bounce of a ray at the vertices $V_{p,q}$ and $V_{u,v}$ on the rough surface.

IV. NUMERICAL RESULTS AND EXPERIMENTAL MEASUREMENTS

In this section, the accuracy of the results obtained by the GTD-RT method proposed for the assessment of optical scattering on rough surfaces is examined by comparison with the results obtained by experimental measurements. The improvement of the accuracy of the results obtained from higher-order GTD-RT is investigated by comparing the scattering patterns evaluated using a second-order to those obtained using the first-order GTD-RT. Also, the dependence of the optical scattering on the surface roughness and its dependence on the refractive index of the medium under

the rough surface are studied. The effect of the resolution of the rough surface model on the accuracy of the evaluated scattering pattern is investigated.

A. Experimental assessment of the accuracy of the GTD-RT method proposed for evaluating scattering from rough surfaces

The GTD-RT method proposed in the present work for the evaluation of the far field pattern due to plane wave scattering on rough surfaces of arbitrary statistical parameters is assessed by comparison with some experimental measurements. The source of the incident plane wave is a light source of $\lambda = 635\text{nm}$. The pattern of radiation from this source is presented in Fig. 4 as measured by the optical power meter model Thorlabs® PM100 with the optical sensor S120B. The experimental setup for measuring the scattering pattern is presented in Fig. 5. The rough sheet subjected to the incident beam is placed on a vertical wall. The light source is oriented so that the incident beam makes an angle of 45° with the normal to the sheet. The optical sensor connected to the power meter rotates from $-90°$ to $90°$ with the normal to the sheet to read the intensity of the light scattered from the flat sheet under test. Two white sheets of different roughness degrees are used for assessment of the proposed numerical technique: a glossy white sheet of roughness, $R_D = 0.09$, and a matte white sheet of roughness, $R_D = 0.225$.

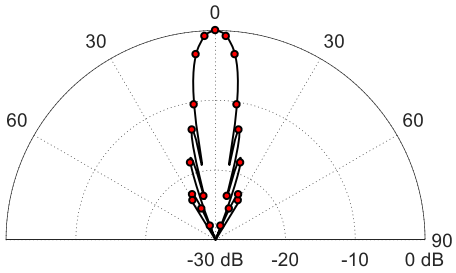

Fig. 4. Radiation pattern of the light beam used for experimental measurements, $\lambda = 635$ nm.

Fig. 5. Experimental setup for measuring the scattering pattern due to a light beam incident on a sheet of rough surface using 635 nm laser source and Thorlabs® optical power meter model PM100 with optical detector model S120B.

A flat sheet of surface roughness, $R_D = 0.09$ is illuminated using the light beam shown in Fig. 5. The optical scattering pattern is measured using the optical power meter through the experimental setup as described above. The measured scattering pattern is compared with that obtained using the second-order GTD-RT method proposed in the present work as shown in Fig. 6 (a). Due to the low degree of roughness of the reflecting surface the scattering pattern shows both specular and diffuse reflection properties. The agreement of the measured pattern with that numerically assessed shows the accuracy of the proposed GTD-RT method for evaluation of scattering of plane waves on rough surfaces. The same experiment is repeated for a flat sheet of surface roughness $R_D = 0.225$. The measured scattering pattern is compared with that obtained using the second-order GTD-RT method proposed in the present work as shown in Fig. 6 (b). For the application of the GTD-RT, the correlation length of the rough surface model is assumed to be $L_C = 7.16$ μm. Both the calculated and measured scattering pattern show diffuse reflection property of the reflecting surface due to the high degree of roughness. The measured scattering pattern agrees with that numerically assessed showing good accuracy of the proposed GTD-RT method.

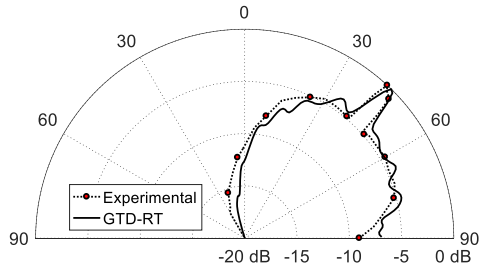

(a) Glossy white sheet of $R_D = 0.09$

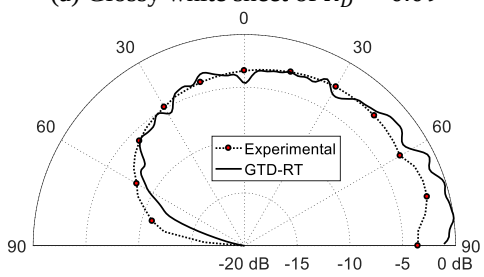

(b) Matte white sheet of $R_D = 0.225$

Fig. 6. Comparison between the scattering patterns obtained through experimental measurements and GTD-RT method for V-polarized optical plane wave of $\lambda = 635$ nm incident on flat white sheets of different values of the roughness, $L_C = 7.16$ μm, $\theta_i^{(n)} = 45°$.

B. Dependence of the scattering pattern on the surface roughness

As experimentally demonstrated, in Section 4.1 the electromagnetic scattering from a surface of medium

roughness exhibits both specular and diffuse properties whereas a highly rough surface causes only diffuse scattering. The scattering pattern for a rough surface is strongly dependent on the surface roughness as shown in Fig. 7 for different values of the angle of incidence. It is clear that the beam width of the scattered optical power increases with increasing the roughness degree. For low roughness ($R_D = 0.01$), the scattering pattern has a high narrow peak in the specular direction determined by Snell's law and insignificant diffuse scattering over the upper space. With increasing the surface roughness ($R_D = 0.05, 0.1$) the diffuse scattering increases whereas the specular scattering decreases and, hence, the scattered beam is broadened and the peak in the specular direction is weakened. For high degrees of roughness, ($R_D = 0.15$), the rough surface produces nearly complete diffuse scattering where the peak due to specular scattering is almost diminished. Also, it is clear that the angle of incidence affects the shape and width of the scattering pattern, where the specular component of the scattered beam seems to be greater with increasing the angle of incidence for a given value of the surface roughness. In the meantime, the backscatter decreases with increasing the angle of incidence for a given value of the surface roughness. Generally, with increasing the surface roughness, irrespective of the angle of incidence $\theta_i^{(n)}$, the backscattered field is clearly increased.

C. Dependence of the accuracy of the calculated scattering pattern on the resolution of the rough surface model

To get accurate results for the scattering coefficients in the far zone using GTD-RT due to a plane wave incident on a rough surface, the number of the incident rays should be large enough to get accurate ray representation of the scattered power distribution over the half-space. The larger the number of incident rays the more accurate the obtained scattering coefficients. As the number of the incident rays is equal to the number of vertices on the rough surface, high resolution of the rough surface is required to get accurate results for the scattering coefficients in the different directions. The case of a surface of roughness $R_D = 0.1$ combines the properties of both diffuse and specular reflections. For this reason, such a roughness is considered to examine the effect of the rough surface resolution on the accuracy of the results obtained for the scattering pattern.

Figure 8 shows the scattering patterns obtained due to a vertically polarized plane incident on a rough surface model with different resolutions (number of vertices constructing its geometric model). For low resolution model (250×250), the scattering pattern seems to have large errors especially in the direction normal to the rough surface and in the specular direction. With increasing the resolution, the accuracy is improved asymptotically (especially in the specular direction) to get very accurate results for a rough surface model of resolution (3000×3000).

D. Dependence of the scattering on the polarization of incident field

The scattering of either H-polarized or V-polarized plane wave incident on a rough surface which is an interface between the free space and a dielectric medium is investigated for different values of the surface roughness and refractive indices. As shown in Fig. 9 (a), for high value of the refractive index ($n = 10$), the scattering patterns for the H-polarized and the V-polarized waves are very close to each other. As shown in Fig. 9 (b), Fig. 10 (a) and Fig. 10 (b) for lower values of the refractive index ($n = 3.16$, $n = 1.5$), respectively, the scattering patterns for the two polarizations are different from each other. It is clear that decreasing the refractive index has the effect of increasing the backscattering of the V-polarized wave and increasing the scattering of the H-polarized wave in the forward direction parallel to the surface.

Increasing the roughness of the surface has the effect of decreasing the specular scattering on behalf of the diffuse scattering for both types of polarization, which is clean by comparison between the scattering pattern presented in Fig. 10 (a) and Fig. 10 (b).

V. COMPUTATIONAL PERFORMANCE OF THE HIGHER-ORDER GTD-RT IN COMPARISON TO THE FIRST-ORDER GTD-RT

The aim of the present section is to investigate the computational complexity and the accuracy of the results obtained by the first and higher-order GTD-RT proposed in the present work.

A. Accuracy of the results

The computational cost of applying second-order GTD-RT is considerably large when compared to that of the first-order GTD-RD. The purpose of the present section is to compare the improvement of the solution obtained using the second-order GTD-RT over that obtained using the first-order method. For this purpose, three ensembles of rough surface models with different statistical parameters are generated. The ensemble has 20 different samples of rough surfaces generated with the same statistical parameters. The rough surface models of the first, second and third ensembles have roughness degrees $R_D = 0.06, 0.10$, and 0.15, respectively where the correlation length is $L_C = 7.16\ \mu m$. For these three ensembles, Figs. 11 (a), (b) and (c), show the scattering patterns resulting due to a plane wave incident at angle $45°$ with the normal to the surface. It is clear that, in all the cases, the improvement due to the application of the second-order GTD-RT can be negligible even for high degrees of roughness.

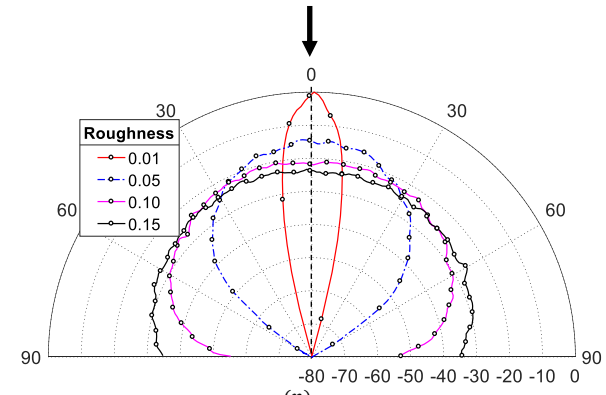

(a) $\theta_i^{(n)} = 0°$

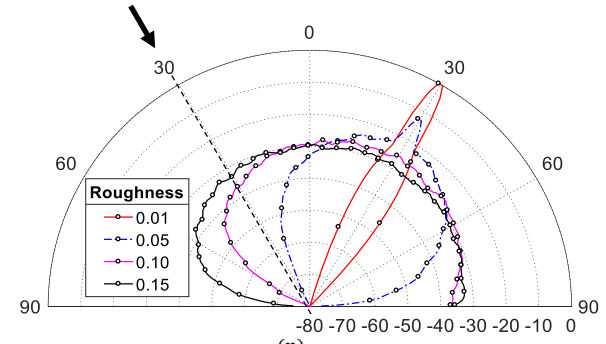

(b) $\theta_i^{(n)} = 30°$

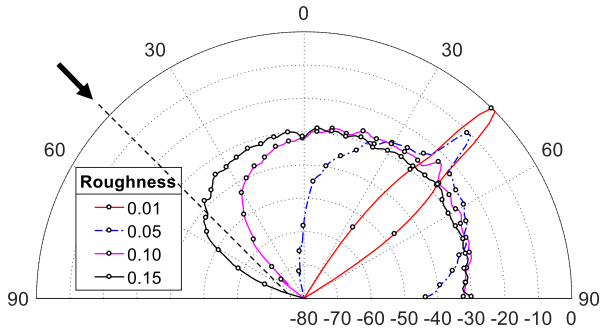

(c) $\theta_i^{(n)} = 45°$

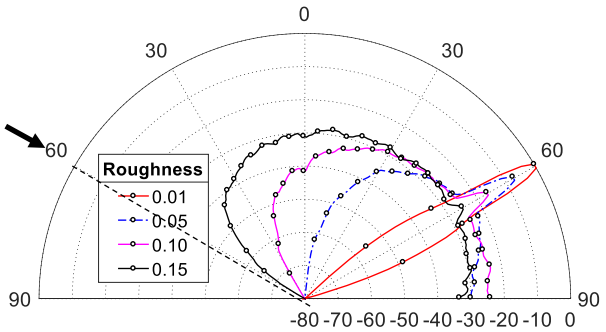

(d) $\theta_i^{(n)} = 60°$

Fig. 7. The scattering patterns due to V-polarized plane wave incident on a rough surface model of resolution 1000×1000, $L_C = 7.16$ μm with different values of the degree of roughness and the angle of incidence.

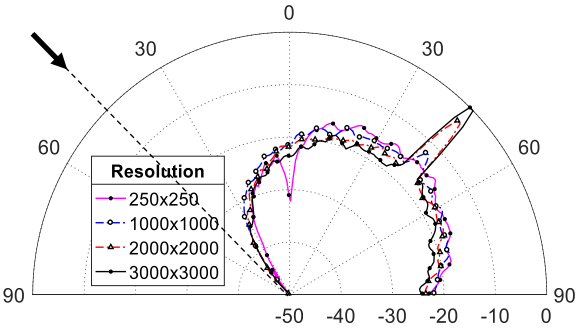

Fig. 8. The scattering patterns due to V-polarized plane wave incident in the direction $\theta_i^{(n)} = 45°$ on a 63.5×63.5 μm rough surface model of different resolutions; $R_D = 0.1$; $\lambda = 635$ nm, $L_C = 7.16$ μm.

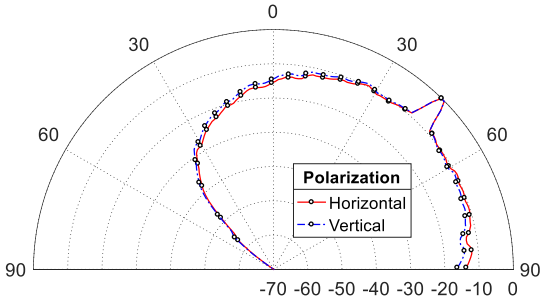

(a) $n = 10$

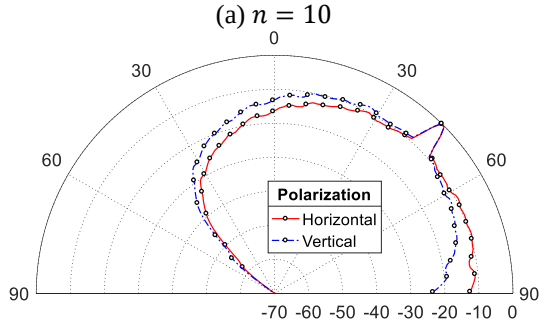

(b) $n = 3.16$

Fig. 9. The scattering patterns due to H-polarized and V-polarized plane waves incident in the direction $\theta_i^{(n)} = 45°$ on a 63.5×63.5 μm rough surface of resolution 1500×1500 vertices and $R_D = 0.10$; $\lambda = 635$ nm, $L_C = 7.16$ μm.

Considering that the results obtained by the second-order method are more accurate than those obtained by the first-order method, Fig. 12 shows the percentage difference between the scattered fields obtained using the two methods averaged over all the directions of the half space for different values of the surface roughness. It is clear that the error due to the application of the first-order RT instead of the second-order RT increases with increasing the surface roughness. However, even for highly rough surfaces (RD = 0.3), the percentage error does not exceed 2.5%. As the application of the second

or higher-order GTD-RT is computationally complex, the negligible improvement of the accuracy over the first-order GTD-RT makes the latter be more efficient for evaluating optical scattering from rough surfaces.

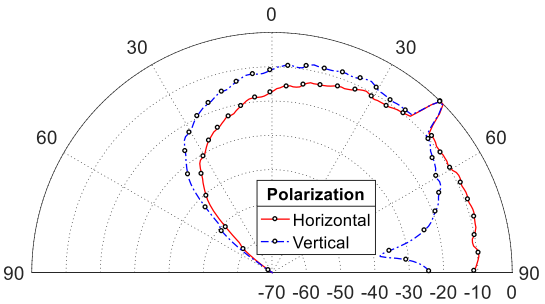

(a) $R_D = 0.10$

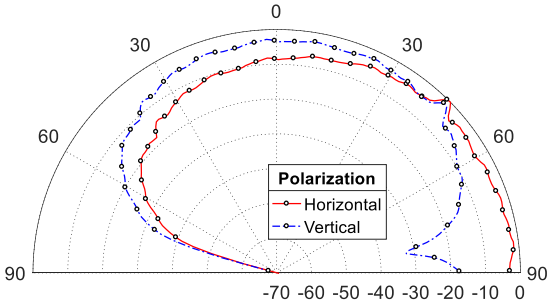

(b) $R_D = 0.15$

Fig. 10. The scattering patterns due to H-polarized and V-polarized plane waves incident in the direction $\theta_i^{(n)} = 45°$ on a 63.5×63.5 μm rough surface of resolution 1500×1500 vertices; $\lambda = 635$ nm, $L_C = 7.16$ μm, $n = 1.5$.

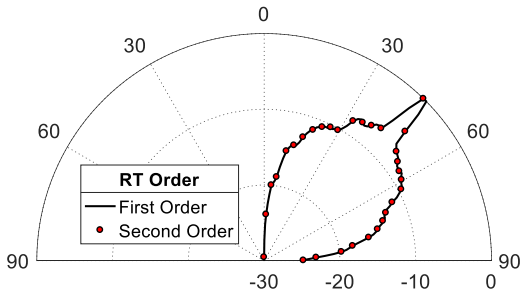

(a) Scattering patterns, $R_D = 0.06$

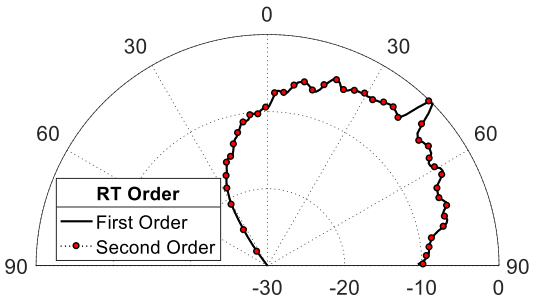

(b) Scattering patterns, $R_D = 0.1$

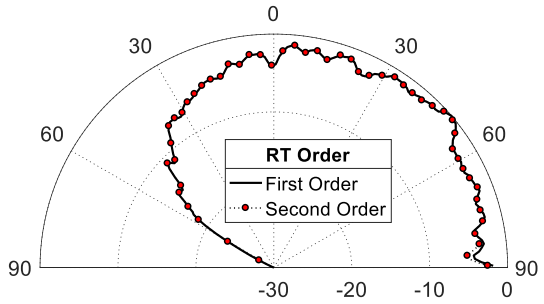

(c) Scattering patterns, $R_D = 0.15$

Fig. 11. The scattering of V-polarized optical plane wave of $\lambda = 635$ nm incident on rough surfaces of $L_C = 7.16$ μm, $\theta_i^{(n)} = 45°$, evaluated by the application of first-order and second-order GTD-RT.

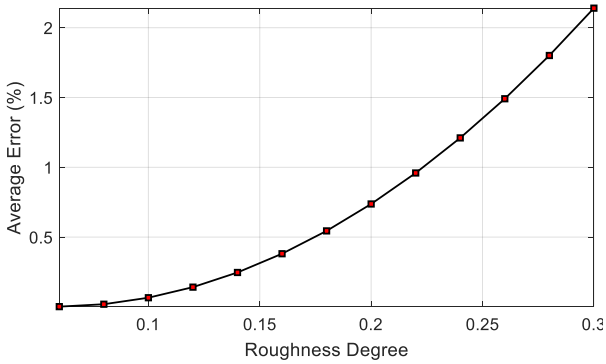

Fig. 12. Average error resulting from the application of the application of the first-order RT relative to the solution obtained by the second-order RT against the degree of roughness. For Simulation, the rough surface has the dimensions 63.5×63.5 μm and the resolution of segmentation is 1000×1000 vertices; $L_C = 7.16$ μm, $n = 1.5$, $\lambda = 635$ nm.

B. Computational time

The dependencies of the computational time and the corresponding percentage error in the magnitude of the backscattered field on the surface roughness are presented in Fig. 13 when applying the first, second and third-order GTD-RT.

It is shown that for the first-order RT, the computational time is slightly decreased with increasing the roughness degree. With increasing the surface roughness, more rays of the incident wave are blocked by the rough surface and, hence, the total number of rays to be traced is further reduced leading to a slight reduction of the computational time. On the contrary, for second-order RT, the possibility of a ray to suffer multiple bounces on the rough surface increases with increasing the surface roughness leading to considerable increase of the computational time. On the other hand, irrespective of the RT order, the percentage error of the

backscatter field magnitude increases with increasing the degree of roughness. With increasing the surface roughness a higher-order order RT is required to keep the solution accurate.

It can be seen from Figs. 13 (a), (b) that for roughness degree of about 0.225, the computational time taken by the second-order RT is about 100 s, which is twice that taken by the first-order RT (50 s). However, the computational error is improved from 3.6% to 2.9% due to the application of the second-order RT instead of the first-order RT.

Thus, the computational time is doubled whereas the error is improved by only 0.7% due to the application of the second-order RT instead of the first-order RT.

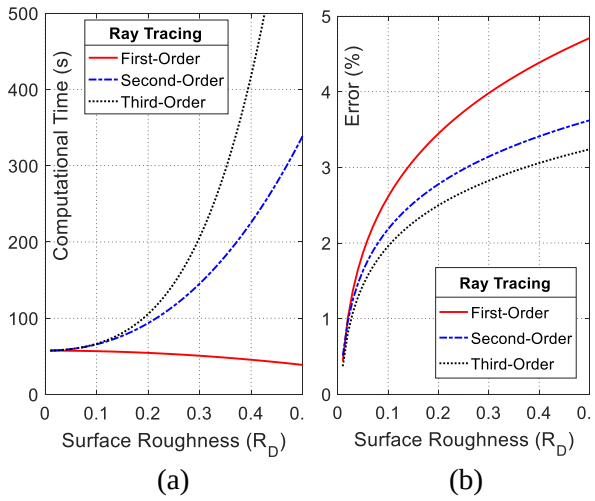

Fig. 13. Dependence of (a) the computational time, and (b) the corresponding percentage error in the magnitude of the backscattered field on the surface roughness.

C. Rate of convergence of ensemble-averaged backscattering with the ensemble size

One of the metrics that is commonly used to assess the computational performance of a numerical method that depends on set of random samples (an ensemble) is the minimum number of samples required to get accurate results after making ensemble averaging. In our case, the ensemble is a set of rough surface models with the same statistical properties. Each of these rough surface samples is subjected to a plane wave to evaluate the scattered field using the GTD-RT proposed in the present work. Then an ensemble averaging is carried out to get the average scattered field. This is known as a Mote-Carlo averaging process. Figure 14 shows the dependence of the ensemble average of the backscattered coefficients for a vertically polarized wave incident on a rough surface with the indicated parameters for different values of the surface roughness. For a rough surface with $R_D = 0.09$, the ensemble-averaged backscattering coefficient is settled down at -20 dB whereas, for a rough surface with $R_D = 0.09$, the ensemble-averaged backscattering coefficient is settled down at -5 dB. In both cases the ensemble average of the backscattered field has fast convergence with the ensemble size. This reflects the efficiency of the proposed GTD-RTD and the perfectness of the rough surface models of the ensemble.

Direction of incidence of the optical wave is $\theta_i^{(n)} = 45°$. For Simulation, the rough surface has the dimensions 63.5×63.5 μm and the resolution of segmentation is 1000×1000 vertices; $L_C = 7.16$ μm, $n = 1.5$, $\lambda = 635$ nm. The reference solution to which the errors are referred to is obtained by experimental measurements

Also, it is shown that the rate of convergence of the ensemble average depends on the surface roughness. For surface roughness $R_D = 0.09$, an ensemble size of 10 samples can be enough to get accurate results, whereas, for $R_D = 0.225$, an ensemble size of 15 samples is required to get accurate results. Thus, the rate of convergence of the ensemble average increases with decreasing the surface roughness.

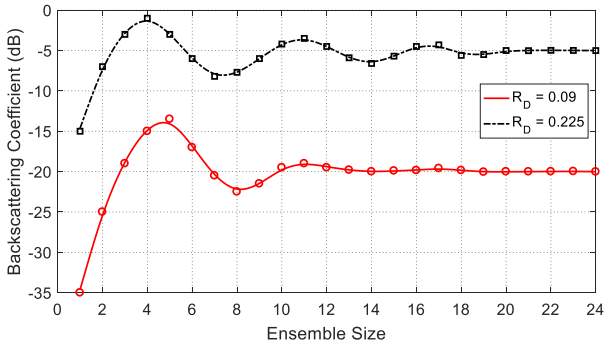

Fig. 14. Convergence of the ensemble-averaged backscattering coefficient with increasing the ensemble size for different values of the surface roughness. Direction of incidence of the optical wave is $\theta_i^{(n)} = 45°$. For Simulation, the rough surface has the dimensions 63.5×63.5 μm and the resolution of segmentation is 1000×1000 vertices; $L_C = 7.16$ μm, $n = 1.5$, $\lambda = 635$ nm.

D. Novelty of the proposed GTD-RT technique

The novelty of the propose GTD-RT technique for the assessment of scattering of plane waves on rough surfaces can be highlighted as follows:

- The method of illuminating the rough surface by the incident power is novel and computationally efficient. This method uses a number of incident rays equal to the number of vertices on the rough surface model. Thus, no intersection points are required to be calculated which saves considerable time.
- Novel and computationally efficient method of calculating shadowing effects of the rough surface. The blocked rays are not considered in the subsequent ray

tracing, which leads to significant improvement of the computational time.
- Novel and computationally efficient algorithm for considering the rays subjected to multiple bounces on the rough surface as described in detail in Section III.B.5.

The samples of the rough surface are perfectly generated using the method described in [27] which leads to fast convergence of the ensemble averaging process. It is found that a number of 10-15 (small-size ensemble) can be enough to get accurate results.

VI. CONCLUSION

The GTD-RT technique is proposed to evaluate the electromagnetic scattering from a rough surface of quite arbitrary statistical parameters. The method of generating the geometrical model of the rough surface is explained. The Fresnel reflection model is applied for arbitrary electrical and optical properties of the rough surface material taking into account the polarization of the incident plane wave. The algorithm developed in the present work can be considered a higher order GTD-RT that accounts for multiple bounces of an incident ray. The accuracy of the obtained results is verified through the comparison with the experimental measurements of the scattering pattern of a light beam incident on samples of rough sheets with specific statistical properties. The presented numerical results are concerned with studying the dependence of the resulting scattering pattern on the surface roughness, refractive index, angle of incidence, and the resolution of the geometric model of the rough surface. Also, it is shown that, for limited resolution of the rough surface model, the accuracy of the calculated scattered field depends on the angle of incidence of the primary beam and the surface roughness.

REFERENCES

[1] A. Manallah and M. Bouafia, "Application of the technique of total integrated scattering of light for micro-roughness evaluation of polished surfaces," *Physics Procedia*, vol. 21, pp. 174-179, 2011.

[2] T. A. Germer, "Polarized light diffusely scattered under smooth and rough interfaces," *Polarization Science and Remote Sensing, International Society for Optics and Photonics*, vol. 5158, pp. 193-205, Dec. 2003.

[3] N. Pinel, C. Bourlier, and J. Saillard, "Degree of roughness of rough layers: Extensions of the Rayleigh roughness criterion and some applications," *Progress in Electromagnetics Research*, vol. 19, pp. 41-63, 2010.

[4] V. A. Ruiz-Cortés and J. C. Dainty, "Experimental light-scattering measurements from large-scale composite randomly rough surfaces," *JOSA A*, vol.

[5] 19, no. 10, pp. 2043-2052, 2002.

[6] A. Manallah and M. Bouafia, "Application of the technique of total integrated scattering of light for micro-roughness evaluation of polished surfaces," *Physics Procedia*, vol. 21, pp. 174-179, 2011.

[7] M. F. Spencer and M. W. Hyde IV, "Rough surface scattering for active-illumination systems," *SPIE Newsroom*, pp. 1-2, 2013.

[8] G. R. Jafari, S. M. Mahdavi, A. Iraji Zad, and P. Kaghazchi, "Characterization of etched glass surfaces by wave scattering," *Surface and Interface Analysis: An International Journal Devoted to the Development and Application of Techniques for the Analysis of Surfaces, Interfaces and Thin Films*, vol. 37, no. 7, pp. 641-645, 2005.

[9] M. Zamani, F. Shafiei, S. M. Fazeli, M. C. Downer, and G. R. Jafari, "Analytic height correlation function of rough surfaces derived from light scattering," *Physical Review E*, vol. 94, no. 4, p. 042809, 2016.

[10] M. Sanamzadeh, L. Tsang, J. T. Johnson, R. J. Burkholder, and S. Tan, "Scattering of electromagnetic waves from 3D multilayer random rough surfaces based on the second-order small perturbation method: Energy conservation, reflectivity, and emissivity," *JOSA A*, vol. 34, no. 3, pp. 395-409, 2017.

[11] Z. S. Wu, J. J. Zhang, and L. Zhao, "Composite electromagnetic scattering from the plate target above a one-dimensional sea surface: Taking the diffraction into account," *Progress in Electromagnetics Research*, vol. 92, pp. 317-331, 2009.

[12] L. Guo, and Z. Wu, "Application of the extended boundary condition method to electromagnetic scattering from rough dielectric fractal sea surface," *Journal of Electromagnetic Waves and Applications*, vol. 18, no. 9, pp. 1219-1234, 2004.

[13] H. H. Qamar, K. F. A. Hussein, and M. B. El-Mashade, "Assessment of signal strength in indoor optical wireless communications using diffuse infrared radiation," *2019 36th National Radio Science Conference (NRSC). IEEE*, 2019.

[14] J. E. Harvey, J. J. Goshy, and R. N. Pfisterer, "Modeling stray light from rough surfaces and subsurface scatter," *Reflection, Scattering, and Diffraction from Surfaces IV. International Society for Optics and Photonics*, vol. 9205, p. 92050I, Sep. 2014.

[15] P. Beckmann, "Scattering by composite rough surfaces," *Proceedings of the IEEE*, vol. 53, no. 8, pp. 1012-1015, 1965.

[16] M. W. Hyde, S. Basu, M. F. Spencer, S. J. Cusumano, and S. T. Fiorino, "Physical optics solution for the scattering of a partially-coherent wave from a statistically rough material surface," *Optics Express*, vol. 21, no. 6, pp. 6807-6825, 2013.

[17] T. M. Elfouhaily and C. A. Guérin, "A critical

survey of approximate scattering wave theories from random rough surfaces," *Waves in Random Media*, vol. 14, no. 4, R1-R40, 2004.

[18] S. O. Rice, "Reflection of electromagnetic waves from slightly rough surfaces," *Communications on Pure and Applied Mathematics*, vol. 4, no. 2-3, pp. 351-378, 1951.

[19] J. Tian, J. Tong, J. Shi, and L. Gui, "A new approximate fast method of computing the scattering from multilayer rough surfaces based on the Kirchhoff approximation," *Radio Science*, vol. 52, no. 2, pp. 186-193, 2017.

[20] E. I. Thorsos, "The validity of the Kirchhoff approximation for rough surface scattering using a Gaussian roughness spectrum," *The Journal of the Acoustical Society of America*, vol. 83no. 1, pp. 78-92, 1988.

[21] M. A. Demir and J. T. Johnson, "Fourth-and higher-order small-perturbation solution for scattering from dielectric rough surfaces," *JOSA A*, vol. 20, no. 12, pp. 2330-2337, 2003.

[22] R. L. Voti, G. L. Leahu, S. Gaetani, C. Sibilia, V. Violante, E. Castagna, and M. Bertolotti, "Light scattering from a rough metal surface: Theory and experiment," *JOSA B*, vol. 26, no. 8, pp. 1585-1593, 2009.

[23] T. V. Vorburger, R. Silver, R. Brodmann, B. Brodmann, and J. Seewig, "Light scattering methods," in: R. Leach (Ed.), *Optical Measurements of Surface Topography*, *Springer*, Berlin, pp. 287-311, 2011.

[24] J. A. Sanchez-Gil and M. Nieto-Vesperinas, "Light scattering from random rough dielectric surfaces," *JOSA A*, vol. 8, no. 8, pp. 1270-1286, 1991.

[25] T. Nordam, P. A. Letnes, and I. Simonsen, "Numerical simulations of scattering of light from two-dimensional rough surfaces using the reduced Rayleigh equation," *Frontiers in Physics*, vol. 1, no. 8, 2013.

[26] H. H. Qamar, A. E. Farahat, K. F. A. Hussein, and M. B. El Mashade, "Assessment of scattering of plane waves on optically illuminated area of rough surface," *Progress in Electromagnetics Research*, vol. 86, pp. 77-102, 2020.

[27] H. H. Qamar, M. B. El-Mashade, A. E. Farahat, and K. F. A Hussein, "Convergence of ensemble averaging for optical scattering on rough surfaces using GTD-RT," in *6th International Conference on Advanced Control Circuits and Systems (ACCS) & 2019 5th International Conference on New Paradigms in Electronics & information Technology (PEIT)*, IEEE, pp. 167-175, 2019.

[28] S. A. M. Soliman, A. E. Farahat, K. F. A. Hussein, and A. A. Ammar, "Spatial domain generation of random surface using Savitzky-Golay filter for simulation of electromagnetic polarimetric systems," *Applied Computational Electromagnetics Society Journal*, vol. 34, no. 1, 2019.